scientific reports

OPEN

Tuning of liver circadian transcriptome rhythms by thyroid hormone state in male mice

Leonardo Vinicius Monteiro de Assis [1,2,10], Lisbeth Harder [1,3,10], José Thalles Lacerda [4], Rex Parsons [5], Meike Kaehler [6], Ingolf Cascorbi [6], Inga Nagel [6,7], Oliver Rawashdeh [8], Jens Mittag [9] & Henrik Oster [1,2]

Thyroid hormones (THs) are important regulators of systemic energy metabolism. In the liver, they stimulate lipid and cholesterol turnover and increase systemic energy bioavailability. It is still unknown how the TH state interacts with the circadian clock, another important regulator of energy metabolism. We addressed this question using a mouse model of hypothyroidism and performed circadian analyses. Low TH levels decreased locomotor activity, food intake, and body temperature mostly in the active phase. Concurrently, liver transcriptome profiling showed only subtle effects compared to elevated TH conditions. Comparative circadian transcriptome profiling revealed alterations in mesor, amplitude, and phase of transcript levels in the livers of low-TH mice. Genes associated with cholesterol uptake, biosynthesis, and bile acid secretion showed reduced mesor. Increased and decreased cholesterol levels in the serum and liver were identified, respectively. Combining data from low- and high-TH conditions allowed the identification of 516 genes with mesor changes as molecular markers of the liver TH state. We explored these genes and created an expression panel that assesses liver TH state in a time-of-day dependent manner. Our findings suggest that the liver has a low TH action under physiological conditions. Circadian profiling reveals genes as potential markers of liver TH state.

Thyroid hormones (THs) are important regulators of embryonic development and energy metabolism. Produced in the thyroid gland in response to stimulation of the hypothalamus–pituitary–thyroid axis, thyroxine (T_4) and, to a much lower extent, the biologically active 3,3',5-triiodothyronine (T_3) are secreted into the bloodstream. At target tissues, T_4 is converted into T_3 via specific deiodinases (DIOs). T_3 can bind to the two nuclear TH receptors (THR) alpha/THRA and beta/THRβ which act as transcription factors. As in most tissues, T_3 action in the liver is predominantly exerted by one primary nuclear receptor, in this case, THRβ[1–3].

THs effects in mammals are diverse and highly tissue specific. The thyroid state (i.e., systemic levels THs) profoundly affects energy metabolism with high THs levels correlating with lower body weight and increased thermogenesis, lipolysis, and glucose usage. In the liver, T_3 simultaneously induces *de-novo* lipid biosynthesis and, to a greater extent, lipolysis. Increased liver fatty acid (FA) uptake and turnover through beta-oxidation in mitochondria and peroxisomes are induced by T_3. Similarly, T_3 enhances cholesterol uptake, biosynthesis, and metabolization into bile acids, and it also increases hepatic gluconeogenesis and inhibits glycolysis and acetyl-coA utilization in the tricarboxylic acid (TCA) cycle[1,3,4]. Low THs levels, found in subclinical and clinical

[1]Center of Brain Behavior and Metabolism, Institute of Neurobiology, University of Lübeck, Marie Curie Street, 23562 Lübeck, Germany. [2]University Hospital Schleswig-Holstein, Campus Lübeck, Lübeck, Germany. [3]Present address: Division of Molecular Neurobiology, Department of Medical Biochemistry and Biophysics, Karolinska Institutet, Stockholm, Sweden. [4]Department of Physiology, Institute of Bioscience, University of São Paulo, São Paulo, Brazil. [5]Faculty of Health, School of Public Health and Social Work, Australian Centre for Health Services Innovation and Centre for Healthcare Transformation, Queensland University of Technology, Kelvin Grove, Australia. [6]Institute of Experimental and Clinical Pharmacology, University Hospital Schleswig-Holstein, Campus Kiel, Kiel, Germany. [7]Institute of Human Genetics, University Hospital Schleswig-Holstein, Campus Kiel, Kiel, Germany. [8]Faculty of Medicine, School of Biomedical Sciences, University of Queensland, Brisbane, Australia. [9]Center of Brain Behavior and Metabolism, Institute for Endocrinology and Diabetes – Molecular Endocrinology, University of Lübeck, Lübeck, Germany. [10]These authors contributed equally: Leonardo Vinicius Monteiro de Assis and Lisbeth Harder. ✉email: leonardo.deassis@uni-luebeck.de; henrik.oster@uni-luebeck.de

hypothyroidism, are associated with an increased incidence of non-alcoholic fatty liver disease (NAFLD) or Metabolic Dysfunction Associated Steatotic Liver Disease (MASLD)[5–8].

While the general effects of TH on liver metabolism are well-characterized, it remains largely unknown how the thyroid state interacts with the circadian regulation of physiological processes in an organ. Most species have developed endogenous time-keeping mechanisms that allow them to keep track of (day-) time and adjust physiology and behavior in anticipation of regularly recurring events. In mammals, a central clock residing in the hypothalamic suprachiasmatic nucleus (SCN) is reset by the external light–dark cycle and coordinates molecular oscillators in central and peripheral tissues including the liver. At the molecular level, a series of oscillatory inter-locked transcriptional-translational feedback loops comprised of clock genes and proteins oscillate throughout the day, adjusting cellular functions across the 24-h day cycle. Rhythmic factors such as body temperature, hormones (e.g., cortisol and melatonin), and autonomic nervous stimuli are known pathways through which the SCN pacemaker regulates peripheral clocks and rhythms[9,10], but it is still up for discussion how low amplitude rhythmic or arrhythmic signals interact with circadian functions at the tissue level.

We have recently shown that, in mice, a high-TH state leads to marked time-of-day specific alterations in energy metabolism such as increased energy expenditure during the active (i.e., the night) and higher body temperature during the inactive phase (i.e., the day). In the liver, T_3 treatment leads to a rewiring of the diurnal liver transcriptome with strong effects on energy metabolism-associated genes, especially those involved in glucose and lipid metabolism. Transcriptional and metabolite data suggest higher triglyceride biosynthesis during the inactive phase followed by increased lipolysis rates in the active phase in T_3-treated mice. Interestingly, these effects are independent of the liver clock gene machinery itself, which is rather insensitive to T_3 treatment[11].

While the effects of high-T_3 in the liver have been characterized, we investigated here how a low thyroid state affects the circadian regulation of energy metabolism and the liver transcriptome. Low TH levels reduced systemic energy turnover in line with human hypothyroid conditions. At the same time, only modest effects were observed on the liver transcriptome. Circadian transcriptome profiling allowed for more fine-grained characterization of low-TH effects revealing changes in lipid and cholesterol metabolism. Our approach identified several temporally stable TH state-responsive genes that may serve as livers-specific biomarkers of the TH state.

Results

TH state tunes systemic energy metabolism

To model hypothyroid conditions in mice, we supplemented their drinking water with methimazole and potassium perchlorate (MMI group), which suppresses TH biosynthesis through inhibition of thyroperoxidase in the thyroid gland and inhibits iodine uptake[12]. MMI treatment strongly reduced T_3 and T_4 levels and led to strong *Tshb* mRNA induction in the pituitary (Supplmentary Fig. S1A). T_3 levels showed circadian rhythms in the control (CON) and MMI groups peaking in the late and mid-dark phase, respectively (Fig. 1A). T_4, on the other hand, was arrhythmic in both conditions (Fig. 1B; Supplementary file 1).

Reduced food and water intake were observed in MMI compared to CON mice (Supplementary Fig. 1B,C). As had been reported before[13]—and unlike hypothyroid humans—MMI mice had reduced body weight compared to CON mice (Fig. 1C). Compared to CON mice, locomotor activity rhythms were similar in MMI mice, but activity was reduced specifically during the dark phase (Fig. 1D; Supplement Fig. 1D). Body temperature was reduced in MMI during the dark phase (Fig. 1E; Supplementary Fig. 1E). Energy turnover, assessed by oxygen consumption, was slightly lower throughout the day (Fig. 1F; Supplementary Fig. 1F) while respiratory quotient profiles were largely unaltered in MMI mice (Fig. 1; Supplementary Fig. 1G,H).

By averaging profile data over the whole day and comparing data to high-T_3 conditions[11], clear systemic effects of TH state on metabolic homeostasis became apparent. TH state-dependent effects were observed for locomotor activity (r = 0.62, *p* = 0.0191), food intake (r = 0.85, *p* = 0.0002), body temperature (r = 0.75, *p* = 0.0042), and oxygen consumption (r = 0.79, *p* = 0.032, Fig. 1G–J). In sum, our findings confirm that a low TH state decreases systemic energy turnover, but this effect is more pronounced during the dark (active) phase.

Low TH levels have moderate effects on liver transcription

In face of the marked effects of TH state on systemic energy metabolism, we focused our attention on the liver due to its major role as a metabolic organ. We collected tissues every 4 h over the whole day to allow the evaluation of time-of-day dependent effects of TH state on liver transcription. To assess T_3 state effects, we determined differentially expressed genes (DEGs) in T_3 and MMI conditions irrespective of sampling time. Surprisingly, T_3 mice showed a fivefold higher number of DEGs compared to MMI mice (Fig. 2A; Supplementary file 2). DEG analysis was performed separately for each sampling time, and the number of DEGs per timepoint is represented in UpSet plots. DEGs identified for at least one time point yielded 95 DEGs in MMI livers compared to 2200 DEGs (a factor of ca. 23) in high-T_3 mice[11] (Fig. 2B,C; Supplementary file 2). We previously identified 37 robust DEGs, i.e., genes consistently differentially expressed across all time points in high TH liver compared to CON[11]. At a low TH state (MMI), however, no robust DEG was identified (Fig. 2D). Analysis of established liver TH/THR target genes and modulators confirmed a much stronger effect of high-T_3 than low TH conditions on liver TH state (Fig. 2E; Supplementary Fig. 2).

Together, these data show that despite marked systemic effects, MMI treatment had much lower effects on liver transcription. Vice versa, this suggests that, under physiological conditions (CON), the liver is already in a low-TH action.

Diurnal profiling reveals transcriptional effects of a low-TH state in the liver

Evaluation of core clock gene expression profiles showed little effect on rhythmic parameters between MMI and CON mice (Fig. 3A) in line with what was previously observed under high-T_3 conditions[11]. To fully assess the
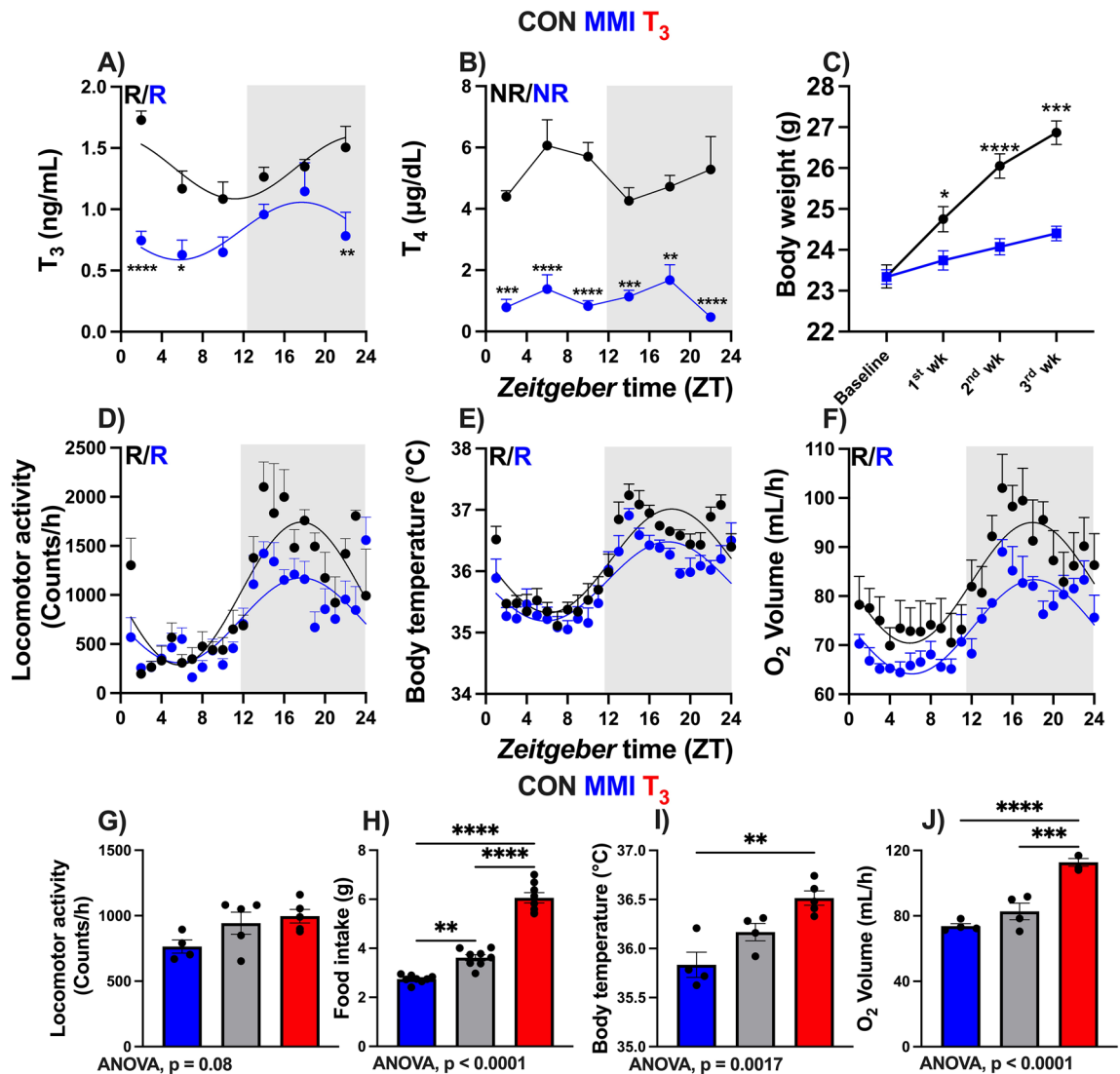
Figure 1. Dose-dependent effects of thyroid hormone (TH) state on systemic energy metabolism. (**A**–**F**) Serum levels of T_3 and T_4, body weight across the experiment, 24-h profiles of locomotor activity, body temperature, and O_2 consumption are shown. Rhythmicity was assessed using CircaCompare algorithm. Presence (R) or absence (NR) of significant circadian rhythmicity is depicted. In the presence of significant 24-h rhythmicity, a sine curve was fit to the data. (**G**–**J**) 24 h average data for locomotor activity, food intake, body temperature, and O_2 consumption for MMI, CON, and T_3[11] groups. One-way ANOVA was performed (p value is shown) followed by Tukey's post-test comparisons (depicted with asterisks). In (**A**) and (**B**), n = 4–6 animals per group or timepoint. In (**C**), n = 24. In (**D**), n = 4 and 5 for CON and MMI groups, respectively. In (**E**) and (**F**), n = 4 for each group. *, **, ***, **** represent a p value of < 0.05, 0.01, 0.001, and 0.0001, respectively.

rhythmic liver transcriptome, the JTK cycle algorithm[14] was used. A total of 3,329 and 3,383 genes (3,354 and 3,397 probe sets) were classified as rhythmic ($p < 0.05$) in CON and MMI, respectively (Supplementary Fig. 3; Supplementary file 3). 1412 genes (1417 probes) were significantly rhythmic in both groups (Supplementary Fig. 3; Supplementary file 3). An average phase delay of 0.24 h was observed for these genes in MMI livers (Fig. 3B) compared to a 1 h phase advance in high-T_3 conditions[11]. Expression peak phases of rhythmic genes were widely distributed, and amplitudes were overall similar between conditions (Supplementary Fig. 3).

To investigate the difference in rhythmic characteristics of the transcriptome regulation under low TH conditions, we performed differential circadian rhythm analysis using CircaCompare[15]. Of the 5297 genes (5334 probes) showing significant 24-h rhythmicity in at least one group, 1882 genes showed changes in mesor, 403 in amplitude, and 391 in phase between low-TH and control conditions (Fig. 4A,B; Supplementary file 4). Processes associated with cellular proliferation, mRNA processing, and macromolecule complex assembly were enriched in genes with mesor DOWN while processes associated with response to oxidative stress and xenobiotic metabolism processes were found in the mesor UP genes. Genes associated with response to hypoxia, exocytosis, and lipid transport showed increased amplitudes in MMI livers. Conversely, the expression of genes involved in oxidative stress and detoxification processes (cellular oxidant detoxification, hydrogen peroxide catabolism, glutathione, and ethanol metabolism) were phase-delayed in MMI mice (Fig. 4C; Supplementary file 4).
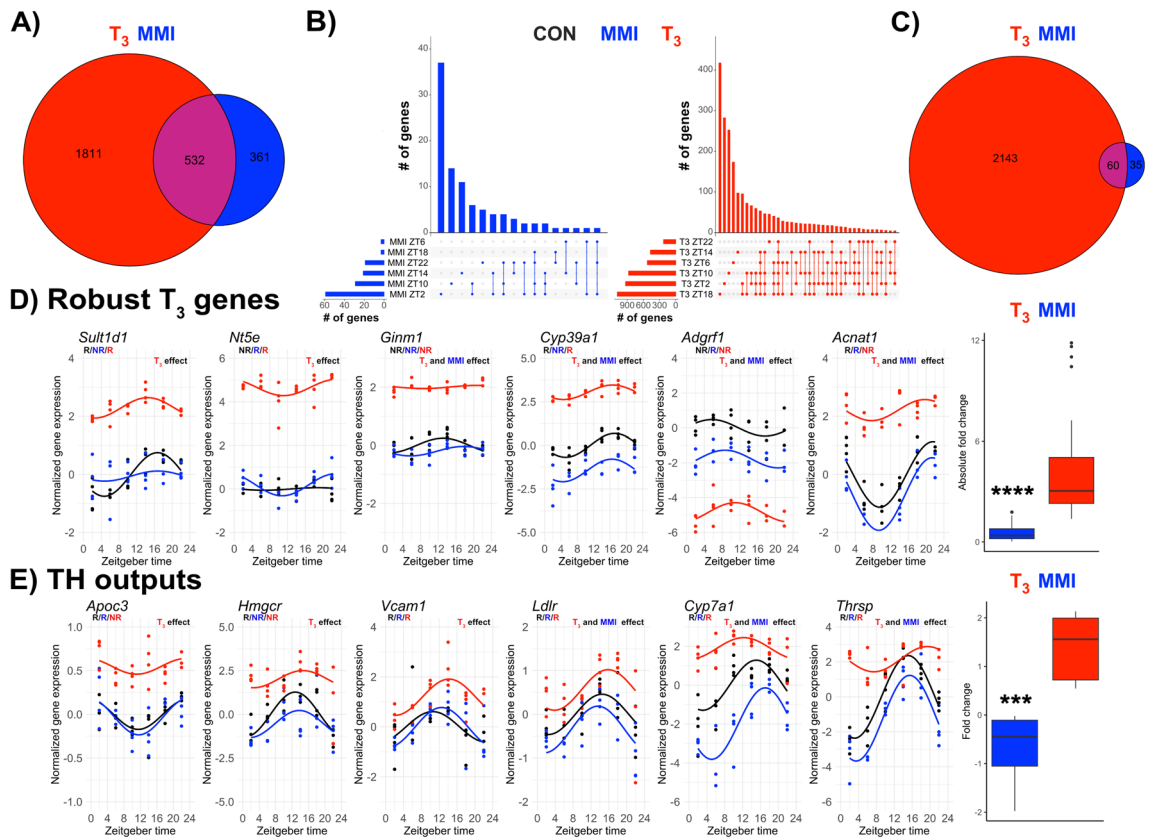
Figure 2. Lowering thyroid hormone state has subtle effects on liver transcriptome rhythms. (**A**) Global DEG analysis (disregarding sampling time) is represented as a Venn diagram. (**B**) UpSet plots represent DEG analysis for each ZT separately. (**C**) Venn diagram represents all temporal DEGs (i.e., showing different expression levels of at least one ZT) identified in MMI and T_3 groups versus CON mice. (**D**) Selected examples of robust DEGs (37 in total) previously identified in T_3-treated mice. Absolute fold change comparison of all 37 DEGs in T_3 and MMI mice are shown. Absolute fold changes were used as some genes were up- or downregulated across the groups. (**E**) Selective TH output genes and fold change of these genes. Comparisons were performed using two-way ANOVA (main treatment effect, $p < 0.05$). n = 3–4 for all ZTs and groups. Pair-wise comparisons were performed by Student's t test with Welch correction. Presence (R) or absence (NR) of circadian rhythm by JTK cycle (p value < 0.05). ***, **** represents a p value of < 0.001, and 0.0001, respectively.

Lipid metabolism-associated processes were regulated for all three rhythm parameters (Fig. 4C). A dual effect (up- and down-regulation) on mesor was observed while most lipid metabolism genes showed reduced amplitudes and phase delays in MMI mice (Fig. 4D). The identified genes were manually inspected and only those genes participating directly in lipid metabolism pathways were included. In this refined gene set for mesor UP, approximately 50% of the genes were associated with acyl-CoA degradation (*Acot1*, *2*, *3*, *4*, *7*, *9*, *13*) and biosynthesis (*Acsm 1*, *3*, *5*) while others were associated with lipolysis (*Lpl*, *Lipa*) and TAG uptake (*Vldr*). In the mesor DOWN group, ca. 40% of the genes were involved in cholesterol biosynthesis (*Aacs*, *Dhcr7*, *Hmgcr*), uptake (*Ldlr*, *Lrp10*, *Npc1*, *Lrp5*, *Pcsk9*), and bile acid secretion (*Abcb11*, *Cyp7a1*, *Abcg5*, *Slc10a1*, *Slc10a5*, *Slc10a2*). Moreover, 35% of the genes were associated with FA biosynthesis (*Acacb*, *Fasn*), elongation (*Elovl1*, *2*, *3*, *5*, *Hacd1*), transport (*Cpt1a*, *Fabp5*), and uptake (*Slc27a2*, *Slc27a5*). Around 30% of amplitude DOWN genes were associated with cholesterol biosynthesis (*Aacs*, *Hsd17b7*) and secretion (*Akr1d1*, *Nr1h5*) while genes with a gain in amplitude were linked with cholesterol uptake (*Abcb1b*) and internal trafficking (*Stard3*, *Npc1*) as well as TAG uptake (*Vldlr*). Genes with expression profile phase effects were more diverse in their functions. Phase-delayed genes were associated with cholesterol metabolization (*Cyp8b1*) and bile acid secretion (*Cyp7a1*, *Abcb11*), FA biosynthesis (*Fads2*), transport (*Cpt1a*) and elongation (*Elovl2*) (Supplementary file 4).

Focusing on cholesterol metabolism, we divided this pathway into three categories: uptake, biosynthesis, and bile acid secretion. Averaged diurnal gene expression from both groups was rhythmic with a strong mesor DOWN effect in MMI mice (Fig. 4E). Total liver cholesterol was reduced and arrhythmic in MMI mice compared to the CON group. On the other hand, serum total cholesterol was elevated in MMI compared to CON mice, indicating impairment in liver cholesterol uptake—as previously suggested. Liver TAG was less responsive to a low-TH state and showed a mesor DOWN effect (Fig. 4F).

Our findings show that a low-TH state results in distinct alterations in liver transcriptome rhythms. Rhythms in lipid and cholesterol metabolism-associated gene programs are affected by low TH levels and translate into differences mostly in cholesterol levels.
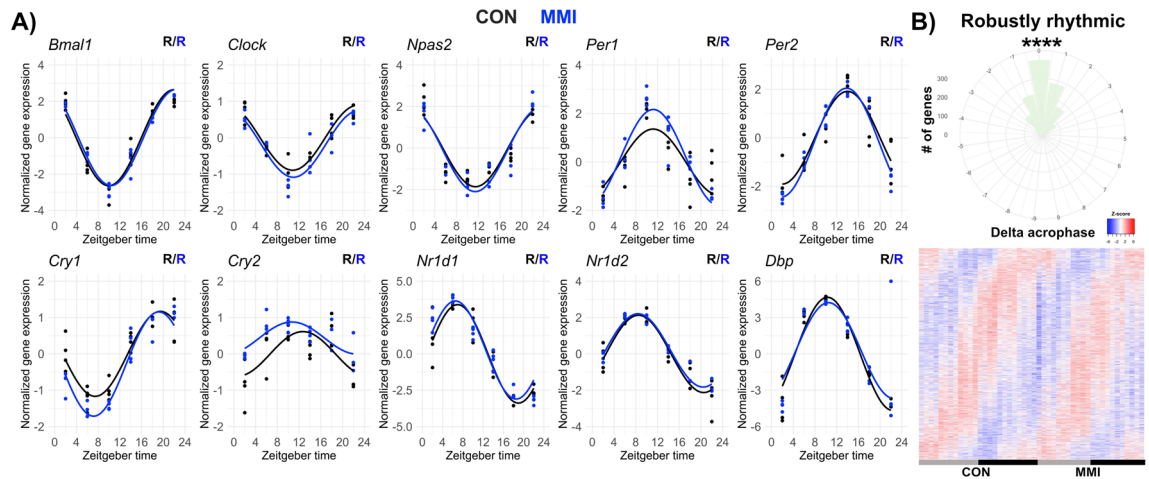
Figure 3. Lowering thyroid hormone state does not affect the rhythmic expression of core clock genes and has a slight phase effect on robustly rhythmic genes. (**A**) Diurnal expression profile of core clock genes is shown. Presence (R) or absence (NR) of significant circadian rhythm by JTK cycle (*p* value < 0.05) is depicted. (**B**) Rose plot and heatmap of robustly rhythmic genes are shown. A minor phase delay of 0.24 h was identified in the MMI group compared to CON (test against zero, *p* < 0.001). n = 3–4 for all ZTs and groups.

Identification of liver TH response genes

When assessing liver TH state across studies—particularly those based in clinical settings—it is not always possible to consider temporal dynamics in liver physiology. Therefore, it would be helpful to identify molecular markers that indicate liver TH state largely independent of sampling time. However, unlike what we had previously shown for high-TH conditions, no robust DEGs were identified in livers of MMI mice (Fig. 2B). While this would preclude reliable data analysis independent of sampling time, we circumvented this limitation by filtering our dataset for transcripts with marked TH state-dependent mesor effects in expression. This would allow for reliable detection of TH state at any time point if sampling time were consistent across experimental conditions. We identified 516 genes that showed consistent mesor effects in response to changes in TH state for both MMI and T_3 conditions (Fig. 5A). Gene Set Enrichment Analysis (GSEA) for genes in the DOWN-MMI/UP-T_3 group showed enrichment for metabolic processes such as steroid, cholesterol, FA, and bile acid metabolism. Conversely, genes in the UP-MMI/DOWN-T_3 group were associated with processes involved in FA, lipoprotein, carbohydrate, and xenobiotic metabolism, amongst others. Interestingly, glucose Glucose/glycogen metabolism was exclusively enriched in the UP in MMI/down in T_3 group (Fig. 5B,C; Supplementary file 5), suggesting a TH-driven overall inhibition of these pathways in line with our previous observations[11]. Averaged expression of all genes pertaining to similar biological processes across the day showed that lipid metabolism—mostly comprised of FA biosynthesis, TAG uptake and biosynthesis—genes were highly responsive to TH levels, being up- and downregulated in T_3 and MMI mice, respectively. Genes associated with FA catabolism were up- and downregulated in MMI and T_3 mice, respectively. As already indicated in the GSEA, cholesterol and bile acid metabolism were markedly affected as MMI and T_3 mice showed down- and upregulation, respectively (Fig. 5C; Supplementary file 5). Validation of selected metabolic genes identified in the microarray was confirmed by qPCR (Supplementary Fig. 4).

Absolute mesor change was used to rank each gene for each comparison (CON *vs.* T3 and CON *vs.* MMI). The top-4 genes (*Tlcd2*, *Stim2*, *Sdr9c7*, *Akr1c19*) are shown (Fig. 5D) recapitulating low or high TH states at any fixed timepoint across the day. Independent qPCR validation confirmed the array findings (Supplementary Fig. 4). The fact that these genes are robustly rhythmic across conditions further emphasizes that sampling time should be kept consistent even in one-timepoint sampling studies (Fig. 5D; Supplementary file 5). To test the predictive efficiency of our approach, we used the published T_3 atlas that combines transcriptome and TH receptor ChipSeq data from different tissues[16]. We identified an overlap of ca. 70% (161 of 224 genes) between the two datasets, further supporting the validity of our approach. We further validated the predictive power of our tuning approach by comparing it against two studies. The first one[17] consisted of rending mice hyperthyroid by supplementing T_4 in the drinking water for two weeks, followed by two weeks of recovery. From the TH-responsive DEGs identified, 42 overlapped with our tuning DEGs (20% overlap). The second study[18] rendered THRβ^{WT} and THRβ^{KO} mice hypothyroid for four weeks, followed by one week of T_3 supplementation. This experiment design allowed the identification of THRβ-responsive genes. From our DEGs tunning set, a total of 128 genes were identified, representing 60% of overlap (Supplementary file 5).

Collectively, the predictive power of the tuning DEG set was validated in public datasets and represents an interesting gene set to estimate TH liver state quantitatively.
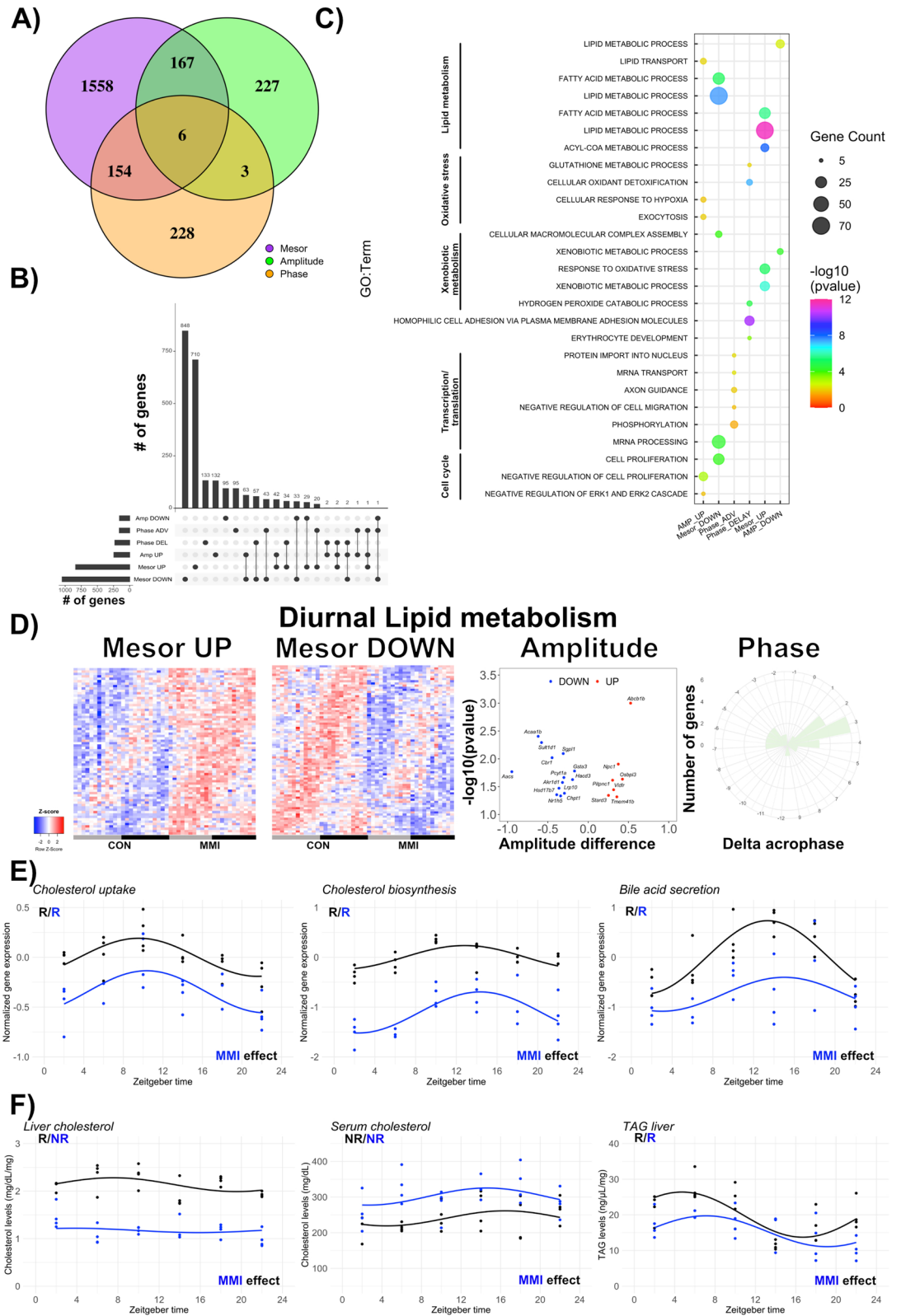
Figure 4. Differential rhythm analysis reveals changes in liver transcriptome rhythms that affect lipid and cholesterol metabolism in MMI mice. (**A**) Differential rhythm analysis was performed using CircaCompare and is represented as Venn diagrams. (**B**) UpSet plots show alterations in diurnal rhythm parameters (mesor, amplitude, phase). (**C**) Gene set enrichment analysis (GSEA) of the genes with either mesor, amplitude, or phase alterations was performed. Top-5 biological processes for each category are shown. (**D**) In-depth diurnal lipid metabolism analysis in response to low thyroid hormone state. Heatmaps show genes with mesor changes. Volcano plot and rose plot show alterations in amplitude and phase, respectively. (**E**) Normalized gene expression of selected genes participating in cholesterol uptake, biosynthesis, and degradation (bile acid secretion) in CON and MMI mice. (**F**) Quantification of cholesterol and TAG in serum or liver. Presence (R) or absence (NR) of significant circadian rhythm by CircaCompare (p value < 0.05) is depicted. n = 3–4 for all ZTs and groups.
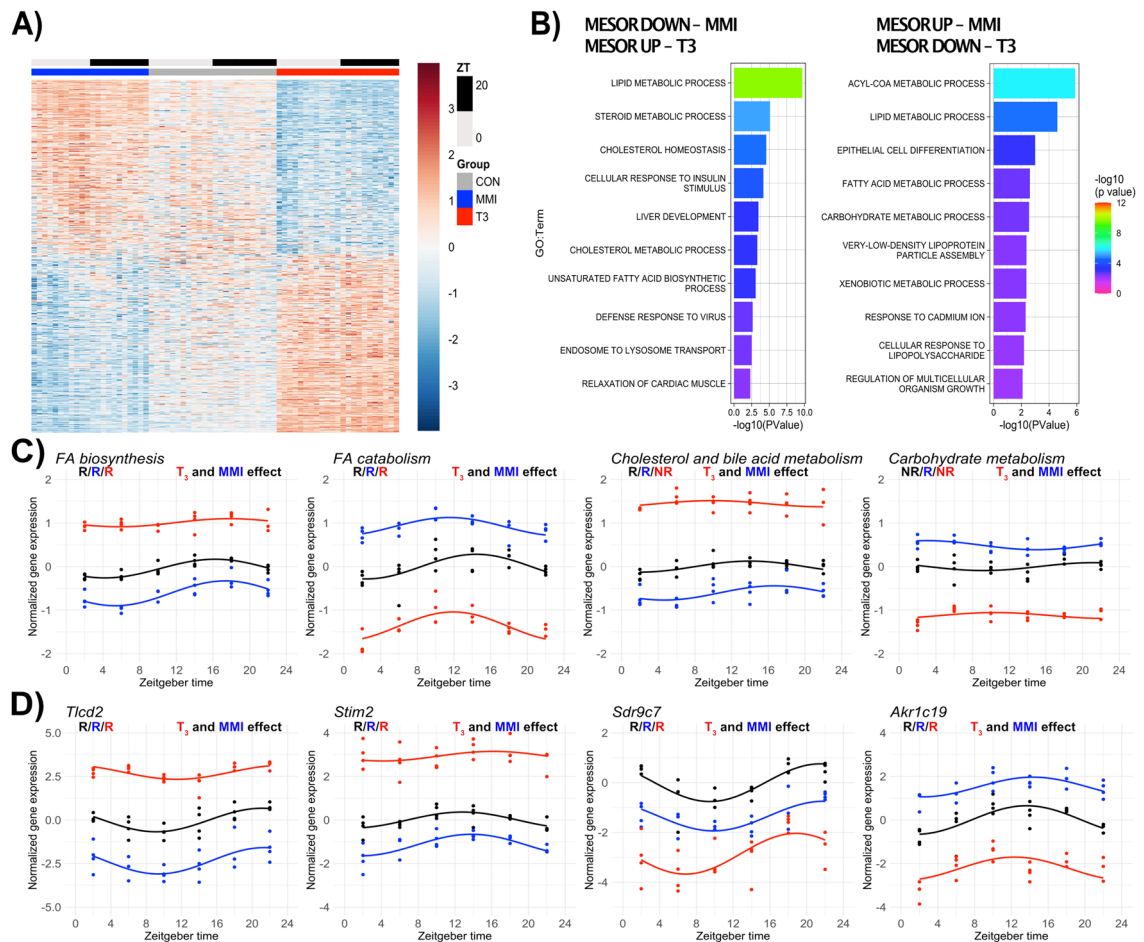
Figure 5. Identification of thyroid hormone-responsive genes by mesor comparison. (**A**) Heatmap shows the 516 TH-dose responsive genes with differential mesor expression among each group. (**B**) Gene set enrichment analysis (GSEA) of mesor-altered genes is shown for each condition. (**C**) Genes pertaining to similar biological pathways identified in B were normalized by CON mesor and plotted. FA biosynthesis pathway comprises lipid metabolic process, unsaturated fatty acid biosynthetic process, long-chain fatty-acyl-CoA biosynthetic process, diacylglycerol biosynthetic process, negative regulation of fatty acid biosynthetic process, and lipid storage. FA catabolism pathway is comprised of acyl-CoA metabolic process, lipid metabolic process, fatty acid metabolic process, very-low-density lipoprotein particle assembly processes. Cholesterol and bile acid metabolism pathways comprise cholesterol homeostasis, cholesterol metabolic process, steroid metabolism, and bile acid signaling pathway. Carbohydrate metabolism pathways are comprised of carbohydrate metabolic process, glycogen metabolic process, ATP metabolic process, and glucose homeostasis. (**D**) Selected biomarkers for TH state at all time points (additional genes can be found in Supplementary file 5). Presence (R) or absence (NR) of circadian rhythm by CircaCompare (p value < 0.05) is depicted. n = 3–4 for all ZTs and groups.

Discussion

In line with the role of TH in metabolic regulation, reducing the TH state by MMI treatment decreased energy turnover in mice. Contrasting these systemic effects, transcriptional responses in the liver were surprisingly subtle with only a few temporally stable DEGs compared to animals with normal or elevated TH levels. Temporal profiling of transcriptome responses, however, revealed time-of-day dependent changes in metabolic pathways in MMI livers. An altered gene signature associated with TAG and cholesterol metabolism was identified. Interestingly, cholesterol levels were more sensitive to a low TH state than TAGs. Compiling our circadian low- and high-TH datasets genes, several biomarker genes for the TH state were identified and could be used to assess the liver TH state robustly.

In MMI mice, T_3 and T_4 levels were markedly suppressed, whereas a strong induction (ca. 40-fold) of pituitary *Tshb* mRNA expression was identified, confirming the success of our experimental approach. The circadian rhythm of T_3 in the blood was retained at low-TH conditions. In line with previous studies in rodents and observations in hypothyroid patients, we identified TH dose- and time-dependent effects on systemic energy metabolism[13,19,20]. Notably, the effects of a low-TH state on energy metabolism were largely restricted to the active phase. MMI mice showed decreased body weight throughout the experiment, contrasting with hypothyroid conditions in humans. These differences were recently confirmed in genetic hypothyroidism mouse models and

are associated with food intake suppression, higher skeletal-muscle adaptive thermogenic and fatty acid oxidation in low-TH mice[13].

Liver transcriptome analyses showed 23-fold fewer DEGs in MMI- compared to T_3-treated (high-TH) mice. This reduced liver responsiveness to a low TH input is further reflected in decreased effects on the established TH/THR target genes[2,4]. Further, THR (*Thra* and *Thrb*) expression in response to TH state alterations was only seen in T_3- but not in MMI-treated animals. In contrast, the expression of *Dio1*, the main deiodinase in the liver[21], showed a clear TH dose-dependent effect. Knockdown of liver *Dio1* favored the development of fatty liver disease (NAFLD/MASLD) due to reduced fatty acid oxidation[22]. Our data suggest that reducing TH action under physiological conditions would be of little consequence as the liver is already a low-TH action organ. An alternative explanation for our findings of low liver responses to reduced TH state would be that intra-liver TH levels could be stabilized due to high DIO1 activity. *Dio1* mRNA was downregulated in the MMI group, which speaks against this idea, but evaluating DIO1 activity or directly measuring liver TH levels would be needed to fully exclude this option.

While these conclusions arise from a simple overall gene expression analysis, circadian profiling of transcriptome data allows for a much more fine-grained evaluation[23]. Previously undetected alterations in several genes revealed novel affected biological processes in response to a low TH state such as cellular proliferation, hypoxia, and oxidative stress, which may serve as hypothesis-generating data for follow-up experiments. We here focused our efforts on lipid metabolism because of the putative role of TH in NAFLD/MASLD regulation[24,25], a condition that also has been linked to circadian rhythms[26,27].

Gene signatures of lipid and cholesterol metabolism showed alterations in all three rhythm parameters (mesor, phase, and amplitude) in MMI-treated mice. Serum cholesterol was highly sensitive to TH state. Increased serum cholesterol levels in MMI mice agreed with previous observations of murine models for sub-clinical[28] or severe hypothyroidism[29]. Diurnal transcriptome profiling showed a mesor DOWN effect in genes associated with cholesterol uptake, biosynthesis, and bile acid secretion. A low TH state is known to reduce bile acid secretion in gall bladder, ileum, and feces compared to euthyroid mice[30] and an increased incidence of cholesterol gallstone formation has been associated with decreased circulating TH levels[31,32]. In contrast, liver TAG levels were less responsive to a low TH state despite marked related alterations at the transcript level. A murine study using a severe hypothyroidism model (low-iodine plus *Slc5a5* knockout) found a protective effect against NAFLD/MASLD. In this model, the hampered TH signaling impairs the adrenergic adipose-derived lipolysis, which reduces fatty acids shuttling to the liver. The reduction of fatty acid uptake by the liver prevents NAFLD/MASLD development. However, a mild hypothyroidism model, achieved by a low iodine diet for 12 weeks, increased liver TAG levels as the adrenergic adipose-derived fatty acid shuttling was not impaired[29]. Increased liver TAG has been reported in a subclinical model of hypothyroidism, achieved by low doses of MMI in drinking water after 16 weeks[28]. However, a recent study using propylthiouracil for 2 and 4 weeks found no changes in TAG and cholesterol levels despite changes in the serum[33].

Our findings show that a low TH state produces transcriptional changes that impair cholesterol metabolization by reducing liver cholesterol uptake, biosynthesis, and bile acid secretion. We suggest that the low cholesterol clearance of MMI mice results in increased serum cholesterol that can be classified as dyslipidemia and an early consequence of a low TH state. Although transcriptional changes associated with TAG metabolism were observed, liver TAG showed a less pronounced alteration and is suggestive of being a late consequence of hypothyroidism.

The systemic changes observed at low thyroid hormone (TH) levels extend beyond the alterations detected in the liver. MMI mice exhibit a decrease in metabolic activity, likely stemming from disrupted metabolic networks across multiple organs. Such a decline in metabolism may reduce the transport of free fatty acids from adipocytes to the liver, impacting lipid synthesis and beta-oxidation processes. Additionally, diminished locomotor activity may lead to lower energy expenditure and reduced consumption of energy resources, contributing to an overall metabolic slowdown. This is mirrored by the lower body temperatures observed in MMI mice. Further research is imperative to understand the responses of other metabolic tissues to a low-TH state and to elucidate the influence of the circadian clock on these interconnected metabolic pathways.

Considering that liver metabolism changes over the course of the day[34,35] and many metabolic genes showed time-of-day dependent responses to low- (this study) or high-[11] TH state, time emerges as an important variable in characterizing metabolic footprints in liver and, potentially, other tissues. We have recently modeled the impact of accounting for time in identifying DEGs in a mouse model of NASH motivated by low consistency in DEG identification in published studies. Accounting for time and using circadian analytical methods led to a ca. sevenfold higher DEG yield[23].

Circadian profiling may not often be feasible—or simply too expensive—particularly in clinical settings. Therefore, we used our data to identify genes that consistently respond to changes in TH state at all times of day as potential robust markers of liver TH state. None of the previously identified 37 high-TH response genes[11] showed altered expression after MMI treatment. In this new approach, time was fully considered yielding markers of TH state in the liver. Rhythmic genes with mesor changes are associated with several metabolic processes known to be TH regulated such as lipid, glucose, steroid, and xenobiotic metabolism. We further explored the mesor-affected genes as possible candidates to estimate liver TH status.

We restricted our analysis to genes that only showed mesor changes to avoid possible confounding factors caused by amplitude and/or phase. In this subset, 224 genes were identified as only being affected at the mesor level. Importantly, out of the 37 robust DEGs identified at high TH conditions, only two genes (*Gstt1* and *Alt2*) were present in MMI mice. Such findings are expected as in this new analysis both rhythmicity and mesor differences were considered. Using public datasets of different experiments that manipulated systemic TH levels, we obtained a good overlap between tuning DEGs and published data, thus demonstrating that our experimental approach can be useful in future experiments to identify and compare liver TH states. Importantly, we did not

identify a 100% overlap between our tuning DEGs and other datasets. This could be associated with using different experimental protocols of low and high TH state induction, sampling time, and/or methodological aspects (ex. RNAseq *vs.* microarray). In addition, our study corroborates these findings by demonstrating that not all genes are equally responsive to TH and can show a gradual response to TH across the day. This is particularly detected in our diurnal analysis and could explain the distinct overlap across the studies.

Our findings show that several thousand T_3-induced DEGs are affected by time, which can directly affect DEG detection if sampling time is inconsistent. However, our findings further refine this dataset and provide a selective set of genes that can be used to establish liver TH state. We suggest that this gene panel can be used to estimate liver TH state if sampling is time-controlled in experimental and possibly clinical studies.

As previously observed in a high-TH condition[11], the circadian core clock was largely unaffected by either low or high T_3 conditions. These findings suggest that TH effects on transcriptome rhythms are downstream of the liver circadian clock and warrant further investigation. Metabolic changes evoked by a low TH state emerged only upon temporal profiling. We also identified a subset of genes that respond in a TH dose-dependent manner with changes in expression mesor. We suggest these genes can be used for follow-up validations of TH liver state in experimental conditions containing limited time points. Understanding the circadian effects of TH state may prove useful for identifying therapeutic targets and optimizing existing treatment strategies for metabolic liver diseases.

Limitations

Our conclusions are drawn from a pharmacological hypothyroidism model. Further validation using genetic models of hypothyroidism to investigate low TH action in the liver should be performed. Due to methodological limitations, all differential rhythm analyses were performed using CircaCompare in a pair-wise fashion without correcting for multiple testing, which could result in increased false positives. We mitigated this limitation by using two different circadian methods to estimate and assess rhythmicity. Our findings suggest that differences can be reliably detected if sampling time is kept consistent. However, performing a circadian profile improves the detection of affected genes and pathways beyond what is achievable through single-timepoint analysis. The hypothyroidism model was successful as evaluated by reduced serum TH levels and increased pituitary *Tshb* expression. Our conclusion that the liver is a low TH action organ arises from the gene signature of known TH targets (e.g., *Thrsp*, *Dio1*, *Cyp7a1*), which suggests a low effect of low compared to a high TH condition. We base our claims on an action standpoint (target gene expression) and not on specifically low intrahepatic TH levels themselves. Further investigation of intrahepatic TH levels is required. Importantly, how male and female mice differ in response to a low and high TH state is a matter for future investigation.

Material and methods
Mouse model and experimental conditions

Two- to three-months-old male C57BL/6 J mice (Janvier Labs, Germany) were housed in groups of three under a 12-h light, 12-h dark (LD, ~ 300 lx) cycle at $22 \pm 2\ °C$ and a relative humidity of $60 \pm 5\%$ with *ad-libitum* access to food and water. Mice were treated with methimazole (MMI, 0.1%, Sigma-Aldrich, USA) potassium perchlorate (0.2%) and sucralose (1 tablet per 50 ml, Tafelsüss, Borchers) for three weeks.

During the treatment period, mice were monitored for body weight individually and food and water intake per cage. All in vivo experiments were ethically approved by the Animal Health and Care Committee of the Government of Schleswig–Holstein and were reported according to the ARRIVE international guidelines. All methods were carried out in accordance with relevant guidelines and regulations. The sample size was calculated using G-power software (version 3.1) and is shown as biological replicates in all graphs.

Euthanasia was carried out using cervical dislocation and tissues were collected every 4 h. Night experiments were carried out under dim red light. Tissues were immediately placed on dry ice and stored at $-80\ °C$ until further processing. Blood samples were collected from the trunk, and clotting was allowed for 20 min at room temperature. Serum was obtained after centrifugation at 2500 rpm, 30 min, 4 °C, and samples stored at $-20\ °C$.

Total T_3 and T_4 evaluation

Serum quantification of T_3 and T_4 was performed using commercially available kits (NovaTec, Leinfelden-Echterdingen, DNOV053, Germany for T_3 and DRG Diagnostics, Marburg, EIA-1781, Germany for T_4) following the manufactures' instructions.

Triglycerides and cholesterol evaluation

TAG and total cholesterol evaluation were processed according to the manufacturer's instructions (Sigma-Aldrich, MAK266 for TAG and Cell Biolabs, San Diego, USA, STA 384 for cholesterol).

Telemetry and metabolic evaluation

Core body temperature and locomotor activity were monitored in a subset of single-housed animals using wireless transponders (E-mitters, Starr Life Sciences, Oakmont, USA). Probes were transplanted into the abdominal cavity of mice 7 days before starting the drinking water treatment. During the treatment period, mice were recorded once per week for at least two consecutive days. Recordings were registered in 1-min intervals using the Vital View software (Starr Life Sciences). Temperature and activity data were averaged over two consecutive days (treatment days: 19/20) and plotted in 60-min bins.

An open-circuit indirect calorimetry system (TSE PhenoMaster, TSE Systems, TSE Systems, USA) was used to determine respiratory quotient (RQ = carbon dioxide produced/oxygen consumed) and energy expenditure in a subset of single-housed mice during drinking water treatment. Mice were acclimatized to the system for one

week prior to starting the measurement. Monitoring of oxygen consumption, water intake as well as activity took place simultaneously in 20-min bins. VO_2 and RQ profiles were averaged over two consecutive days (treatment days: 19/20) and plotted in 60-min bins. Energy expenditure was estimated by determining the caloric equivalent according to Heldmaier[36]: heat production $(mW) = (4.44 + 1.43*RQ)*VO_2$ (ml O_2/h).

Microarray analysis
Total RNA was extracted using TRIzol (Thermofisher, Waltham, USA) and the Direct-zol RNA Miniprep kit (Zymo Research, Irvine, USA) according to the manufacturer's instructions. Genome-wide expression analyses was performed using Clariom S arrays (Thermo Fisher Scientific) using 100 ng RNA of each sample according to the manufacturer's recommendations (WT Plus Kit, Thermo Fisher Scientific). Data were analyzed using Transcriptome Analyses Console (Thermo Fisher Scientific, version 4.0) and expressed in log_2 values. Sample MMI_ZT06_a and MMI_ZT18_d were removed from the data due to low quality.

Quantitative PCR (qPCR)
cDNA was generated by reverse transcription of total RNA using the high-capacity cDNA reverse transcription kit (Applied Biosystems, USA). Gene expression was determined by qPCR using the Go Taq qPCR master mix kit (Promega, USA) and a CFX-96 thermocycler (Bio-Rad, USA). Relative mRNA levels were obtained by analyzing gene expression with the Pfaffl Eq. [37]. *Eef1α* was used as a normalizer due to its robust expression across time and groups. Primer sequences are provided in supplementary file 5.

Differentially expressed gene (DEG) analysis
To identify global DEGs, all temporal data from each group was considered and analyzed by *Student's t* test and corrected for false discovery rates (FDR < 0.1). Up- or downregulated DEGs were considered when a threshold of 1.5-fold (0.58 in log_2 values) regulation was met. As multiple probes can target a single gene, we curated the data to remove ambiguous genes. To identify DEGs at specific time points (ZTs—Zeitgeber time; ZT0 = "lights on"), the procedure described above for each ZT was performed separately. Time-independent DEGs were identified by finding consistent gene expression pattern across all ZTs.

Rhythm analysis
To identify probes that showed diurnal (i.e., 24-h) oscillations, we employed the non-parametric JTK_CYCLE algorithm[14] in the Metacycle package[38] with a set period of 24 h and an adjusted p-value (ADJ.P) cut-off of 0.05. Phase and amplitude parameter estimates from CircaSingle were used for rose plot visualizations[15]. To directly compare rhythm parameters (mesor and amplitude) in gene expression profiles between T_3 and CON, CircaCompare fits were used irrespective of rhythmicity thresholds. Phase comparisons were only performed when a gene was considered as rhythmic in both conditions ($p < 0.05$) as previously described[11]. Temporal profiles were made using geom_smooth (ggplot2 package), method "lm", and formula = y ~ 1 + sin(2*pi*x/24) + cos(2*pi*x/24). Small differences in rhythmic parameters can be present due to the different sine curve fitting between CircaCompare and ggplot curve fit.

Gene set enrichment analysis (GSEA)
Functional enrichment analysis of DEGs was performed using the Gene Ontology (GO) annotations for Biological Processes on the Database for Annotation, Visualization, and Integrated Discovery software (DAVID 6.8[39]). Processes were considered significant for a biological process containing at least 5 genes (gene count) and a *p*-value < 0.05. To remove the redundancy of GSEA, we applied the REVIGO algorithm[40] using default conditions and a reduction of 0.5. For enrichment analyses from gene sets containing less than 100 genes, biological processes containing at least 2 genes were included. Overall gene expression evaluation of a given biological process was performed by normalizing each timepoint by CON mesor.

Data handling and statical analysis of non-bioinformatic related experiments
Samples were only excluded upon technical failure. Data from ZT0-12 were considered as light phase and from ZT 12–24 as dark phase. Day *vs.* night analyzes were performed by averaging the data and comparing using unpaired *Student's* t test with Welch correction. Time-course data were analyzed by Two-way ANOVA for main treatment effects followed by Bonferroni post-test. When applicable, Two-Way for repeated measures was applied. Single timepoint data were evaluated by unpaired *Student's* t test with Welch correction or Mann–Whitney test for parametric or non-parametric samples, respectively. ANOVA One-Way followed by Tukey was used for single timepoint data when CON, MMI, and T_3 groups were evaluated. Spearman's correlation was used for all correlational analyzes. Analyzes were done in Prism 9.4 (GraphPad) and a *p*-value < 0.05 was used to reject the null hypothesis.

Data handling and statical analysis of bioinformatic experiments
Statistical analyses were conducted using R 4.0.3 (R Foundation for Statistical Computing, Austria) or in Prism 9.4 (GraphPad). Rhythmicity was calculated using the JTK_CYLCE algorithm in meta2d, a function of the Meta-Cycle R package v.1.2.0. Rhythmic features were calculated and compared pairwise among the groups using the CircaCompare R package v.0.1.1. Data visualization was performed using the ggplot2 R package v.3.3.5, eulerr R package v.6.1.1, UpSetR v. 1.4.0, pheatmap v. 1.0.12, and Prism 9.4 (GraphPad).

Data availability

References

1. Ritter, M. J., Amano, I. & Hollenberg, A. N. Thyroid hormone signaling and the liver. *Hepatology* **72**, 742–752 (2020).
2. Mullur, R., Liu, Y. Y. & Brent, G. A. Thyroid hormone regulation of metabolism. *Physiol. Rev.* **94**, 355–382 (2014).
3. Sinha, R. A., Singh, B. K. & Yen, P. M. Thyroid hormone regulation of hepatic lipid and carbohydrate metabolism. *Trends Endocrinol. Metab.* **25**, 538–545 (2014).
4. Sinha, R. A., Singh, B. K. & Yen, P. M. Direct effects of thyroid hormones on hepatic lipid metabolism. *Nat. Rev. Endocrinol.* **14**, 259–269 (2018).
5. Elshinshawy, S. *et al.* The interrelation between hypothyroidism and non-alcoholic fatty liver disease, a cross-sectional study. *J. Clin. Exp. Hepatol.* **13**, 638–648 (2023).
6. Kim, D. *et al.* Subclinical hypothyroidism and low-normal thyroid function are associated with nonalcoholic steatohepatitis and fibrosis. *Clin. Gastroenterol. Hepatol.* **16**, 123–131 (2018).
7. Lai, S., Li, J., Wang, Z., Wang, W. & Guan, H. Sensitivity to thyroid hormone indices are closely associated with NAFLD. *Front. Endocrinol.* **12**, 766419 (2021).
8. Ludwig, U. *et al.* Subclinical and clinical hypothyroidism and non-alcoholic fatty liver disease: A cross-sectional study of a random population sample aged 18 to 65 years. *BMC Endocr. Disord.* **15**, 41 (2015).
9. de Assis, L. V. M. & Oster, H. The circadian clock and metabolic homeostasis: Entangled networks. *Cell. Mol. Life Sci. CMLS* https://doi.org/10.1007/s00018-021-03800-2 (2021).
10. Finger, A. M. & Kramer, A. Mammalian circadian systems: Organization and modern life challenges. *Acta Physiol.* https://doi.org/10.1111/apha.13548 (2020).
11. de Assis, L. V. M. *et al.* Rewiring of liver diurnal transcriptome rhythms by triiodothyronine (T3) supplementation. *eLife* **11**, e79405 (2022).
12. Hoefig, C. S. *et al.* Biosynthesis of 3-iodothyronamine from T4 in murine intestinal tissue. *Endocrinology* **156**, 4356–4364 (2015).
13. Kaspari, R. R. *et al.* The paradoxical lean phenotype of hypothyroid mice is marked by increased adaptive thermogenesis in the skeletal muscle. *Proc. Natl. Acad. Sci. USA* **117**, 22544–22551 (2020).
14. Hughes, M. E., Hogenesch, J. B. & Kornacker, K. JTK_CYCLE: An efficient nonparametric algorithm for detecting rhythmic components in genome-scale data sets. *J. Biol. Rhythms* **25**, 372–380 (2010).
15. Parsons, R., Parsons, R., Garner, N., Oster, H. & Rawashdeh, O. CircaCompare: A method to estimate and statistically support differences in mesor, amplitude and phase, between circadian rhythms. *Bioinformatics* **36**, 1208–1212 (2020).
16. Zekri, Y., Guyot, R. & Flamant, F. An atlas of thyroid hormone receptors' target genes in mouse tissues. *Int. J. Mol. Sci.* **23**, 11444 (2022).
17. Nock, S. *et al.* CD5L constitutes a novel biomarker for integrated hepatic thyroid hormone action. *Thyroid* **30**, 908–923 (2020).
18. Shabtai, Y. *et al.* A coregulator shift, rather than the canonical switch, underlies thyroid hormone action in the liver. *Genes Dev.* **35**, 367–378 (2021).
19. Johann, K. *et al.* Thyroid-hormone-induced browning of white adipose tissue does not contribute to thermogenesis and glucose consumption. *Cell Rep.* **27**, 3385-3400.e3 (2019).
20. Yavuz, S., Nunez, S., del Prado, S. & Celi, F. S. Thyroid hormone action and energy expenditure. *J. Endocr. Soc.* **3**(7), 1345–1356 (2019).
21. Luongo, C., Dentice, M. & Salvatore, D. Deiodinases and their intricate role in thyroid hormone homeostasis. *Nat. Rev. Endocrinol.* **15**, 479–488 (2019).
22. Bruinstroop, E. *et al.* Early induction of hepatic deiodinase type 1 inhibits hepatosteatosis during NAFLD progression. *Mol. Metab.* **53**, 101266 (2021).
23. de Assis, L. V. M., Demir, M. & Oster, H. Nonalcoholic steatohepatitis disrupts diurnal liver transcriptome rhythms in mice. *Cell. Mol. Gastroenterol. Hepatol.* **16**, 341–354 (2023).
24. Wirth, E. K., Puengel, T., Spranger, J. & Tacke, F. Thyroid hormones as a disease modifier and therapeutic target in nonalcoholic steatohepatitis. *Expert Rev. Endocrinol. Metab.* **17**, 425–434 (2022).
25. Zhao, M. *et al.* Development of thyroid hormones and synthetic thyromimetics in non-alcoholic fatty liver disease. *Int. J. Mol. Sci.* **23**, 1102 (2022).
26. de Assis, L. V. M., Demir, M. & Oster, H. The role of the circadian clock in the development, progression, and treatment of non-alcoholic fatty liver disease. *Acta Physiol.* **237**, e13915 (2023).
27. Marjot, T., Ray, D. W. & Tomlinson, J. W. Is it time for chronopharmacology in NASH?. *J. Hepatol.* https://doi.org/10.1016/j.jhep.2021.12.039 (2022).
28. Zhou, L. *et al.* Endoplasmic reticulum stress may play a pivotal role in lipid metabolic disorders in a novel mouse model of subclinical hypothyroidism. *Sci. Rep.* **6**, 31381 (2016).
29. Ferrandino, G. *et al.* Pathogenesis of hypothyroidism-induced NAFLD is driven by intra- and extrahepatic mechanisms. *Proc. Natl. Acad. Sci. U S A* **114**, E9172–E9180 (2017).
30. Yan, Y. *et al.* Hepatic thyroid hormone signalling modulates glucose homeostasis through the regulation of GLP-1 production via bile acid-mediated FXR antagonism. *Nat. Commun.* **13**, 6408 (2022).
31. Kube, I. *et al.* Hepatobiliary thyroid hormone deficiency impacts bile acid hydrophilicity and aquaporins in cholestatic C57BL/6J mice. *Int. J. Mol. Sci.* **23**, 12355 (2022).
32. Kube, I. *et al.* Hypothyroidism Increases cholesterol gallstone prevalence in mice by elevated hydrophobicity of primary bile acids. *Thyroid* **31**, 973–984 (2021).
33. Wang, Z. *et al.* Assessing the influence of propylthiouracil and phenytoin on the metabolomes of the thyroid, liver, and plasma in rats. *Metabolites* **13**, 847 (2023).
34. Reinke, H. & Asher, G. Crosstalk between metabolism and circadian clocks. *Nat. Rev. Mol. Cell Biol.* **20**, 227–241 (2019).
35. Reinke, H. & Asher, G. Circadian clock control of liver metabolic functions. *Gastroenterology* **150**, 574–580 (2016).
36. Heldmaier, G. Metabolic and thermoregulatory responses to heat and cold in the *Djungarian hamster, Phodopus sungorus. J. Comp. Physiol.* **102**, 115–122 (1975).
37. Pfaffl, M. W. A new mathematical model for relative quantification in real-time RT-PCR. *Nucleic Acids Res.* **29**, e45 (2001).

38. Wu, G., Anafi, R. C., Hughes, M. E., Kornacker, K. & Hogenesch, J. B. MetaCycle: an integrated R package to evaluate periodicity in large scale data. *Bioinformatics* **32**, 3351–3353 (2016).
39. Huang, D. W., Sherman, B. T. & Lempicki, R. A. Systematic and integrative analysis of large gene lists using DAVID bioinformatics resources. *Nat. Protoc.* **4**, 44–57 (2009).
40. Supek, F., Bošnjak, M., Škunca, N. & Šmuc, T. REVIGO summarizes and visualizes long lists of gene ontology terms. *PloS One* **6**, e21800 (2011).

Acknowledgements

Author contributions

De A.L.V.M.: Data curation, software, formal analysis, investigation, methodology, writing—original draft, writing—review and editing. H.L.: Conceptualization, data curation, formal analysis, investigation, methodology, writing—review and editing. L.J.T., P.R., K.M., C.I., N.I., R.O., Methodology, writing—review and editing. M.J.: Conceptualization, writing—review and editing. O.H.: Conceptualization, supervision, funding acquisition, investigation, writing—original draft, project administration, writing—review and editing.

Funding

Competing interests

The authors declare no competing interests.

Additional information

Supplementary Information The online version contains supplementary material available at https://doi.org/10.1038/s41598-023-50374-z.

Correspondence and requests for materials should be addressed to L.V.M.d.A. or H.O.

Reprints and permissions information is available at www.nature.com/reprints.

Publisher's note Springer Nature remains neutral with regard to jurisdictional claims in published maps and institutional affiliations.